The Cdc42 GTPase-associated proteins Gic1 and Gic2 are required for polarized cell growth in *Saccharomyces cerevisiae*

Guang-Chao Chen, Yung-Jin Kim,[1] and Clarence S.M. Chan[2]

Department of Microbiology, The University of Texas, Austin, Texas 78712 USA

***BEM2* of *Saccharomyces cerevisiae* encodes a Rho-type GTPase-activating protein that is required for proper bud site selection at 26°C and for bud emergence at elevated temperatures. We show here that the temperature-sensitive growth phenotype of *bem2* mutant cells can be suppressed by increased dosage of the *GIC1* gene. The Gic1 protein, together with its structural homolog Gic2, are required for cell size and shape control, bud site selection, bud emergence, actin cytoskeletal organization, mitotic spindle orientation/positioning, and mating projection formation in response to mating pheromone. Each protein contains a CRIB (Cdc42/Rac-interactive binding) motif and each interacts in the two-hybrid assay with the GTP-bound form of the Rho-type Cdc42 GTPase, a key regulator of polarized growth in yeast. The CRIB motif of Gic1 and the effector domain of Cdc42 are required for this association. Genetic experiments indicate that Gic1 and Gic2 play positive roles in the Cdc42 signal transduction pathway, probably as effectors of Cdc42. Subcellular localization studies with a functional green fluorescent protein–Gic1 fusion protein indicate that this protein is concentrated at the incipient bud site of unbudded cells, at the bud tip and mother-bud neck of budded cells, and at cortical sites on large-budded cells that may delimit future bud sites in the two progeny cells. The ability of Gic1 to associate with Cdc42 is important for its function but is apparently not essential for its subcellular localization.**

[*Key Words:* Cellular morphogenesis; cell polarity; GTPase; Cdc42; Bem2]

Received July 11, 1997; revised version accepted September 11, 1997.

Cell growth in the budding yeast *Saccharomyces cerevisiae* is a highly polarized process (for review, see Roemer et al. 1996). Initiation of vegetative growth involves the selection of a nonrandom bud site on the surface of the ellipsoidal cell (Chant and Pringle 1995). After bud emergence, growth occurs initially at or near the bud tip and then later throughout the bud, which becomes the daughter cell after cytokinesis. Under commonly used laboratory culture conditions, **a** or α haploid cells bud mostly from sites near the site of the previous cell division (i.e., axial fashion), whereas **a**/α diploid cells bud in a bipolar fashion, with mother cells that have budded at least once budding from either pole and daughter cells that have never budded budding preferentially from the pole opposite the site of the previous cell division. In response to mating factor, haploid cells also undergo polarized growth by the formation of mating projection. A number of proteins that are required for bud site selection or mating projection formation have been identified (for review, see Roemer et al. 1996).

[1]Present address: Department of Molecular Biology, Pusan National University, Pusan, 609-735, Korea.
[2]Corresponding author.
E-MAIL clarence_chan@mail.utexas.edu; FAX (512) 471-7088.

Once a bud site has been selected, other proteins are required for the subsequent localization of growth to this site (i.e., bud emergence instead of isotropic growth). Of particular interest is the evolutionarily conserved, Ras-related, Rho-type Cdc42 GTPase (Johnson and Pringle 1990), which cycles between the GDP-bound (presumably inactive) and the GTP-bound (presumably active) states. It is regulated by the Cdc24 GDP dissociation stimulator (Bender and Pringle 1989; Zheng et al. 1994; Ziman and Johnson 1994), the Bem3 and Rga1 (Dbm1) GTPase-activating proteins (GAPs) (Zheng et al. 1993, 1994; Stevenson et al. 1995; Chen et al. 1996), and possibly the Zds1 and Zds2 proteins (Bi and Pringle 1996). Conditional *cdc24* and *cdc42* mutant cells are defective in bud emergence and localized cell surface growth, and they become arrested as large, multinucleate, unbudded cells at the restrictive growth temperature (Sloat and Pringle 1978; Sloat et al. 1981; Adams and Pringle 1984; Adams et al. 1990). These cells are also defective in their response to mating factor and thus cannot mate at the restrictive temperature (Simon et al. 1995; Zhao et al. 1995).

Genetic and biochemical studies indicate that Cdc42 and its regulators associate (directly or indirectly) and function together with the bud site selection proteins

Bni1 and Rsr1 (Bud1), thus suggesting that the bud site selection proteins may recruit Cdc42 to selected bud sites, where Cdc42 can perform its function in bud emergence (Bender and Pringle 1989; Ruggieri et al. 1992; Peterson et al. 1994; Zheng et al. 1995; Evangelista et al. 1997; Park et al. 1997). Cdc42, like its mammalian counterparts, functions at least in part to regulate the actin cytoskeleton. *cdc42* mutant cells are defective in the organization of the yeast actin cytoskeleton (Adams and Pringle 1984; Adams et al. 1990; Ziman et al. 1991), and the ability of permeabilized *cdc42* mutant cells to assemble cortical actin patches in vitro is greatly reduced (Li et al. 1995). A functional actin cytoskeleton is important for polarized cell growth because it serves to target secretory vesicles to growth sites (Ayscough et al. 1997). How Cdc42 promotes polarized actin cytoskeletal assembly and bud emergence is unknown. A number of putative effectors of Cdc42 have been identified. Ste20, Cla4, and Skm1 (Cvrcková et al. 1995; Simon et al. 1995; Zhao et al. 1995; Martin et al. 1997) belong to the p21-activated kinase (PAK) family of protein kinases. Ste20 and Cla4 are known to associate with GTP-bound Cdc42, and at least Ste20 becomes activated by this association. Boi1 (and perhaps also its structural homolog Boi2) also associates (directly or indirectly) with GTP-bound Cdc42, but its biochemical properties are unknown (Bender et al. 1996; Matsui et al. 1996).

BEM2 (*IPL2*) encodes a GAP predicted to be specific for Rho-type GTPases (Kim et al. 1994; Peterson et al. 1994). In vitro, the recombinant GAP domain of Bem2 stimulates the GTPase activity of Rho1, but not Cdc42 (Zheng et al. 1993, 1994; Peterson et al. 1994). However, the phenotypes of *bem2* mutant cells are more similar to those of *cdc42* rather than *rho1* mutant cells (Bender and Pringle 1991; Chan and Botstein 1993; Kim et al. 1994; Peterson et al. 1994; Yamochi et al. 1994; Wang and Bretscher 1995). At permissive growth temperatures, conditional *bem2* mutants exhibit randomized bud site selection, whereas at restrictive growth temperatures, these mutants are defective in bud emergence and become arrested as large, round, multinucleate cells that are mostly unbudded. Furthermore, loss of Bem2 function can be compensated by specific alterations in the Rga1 (Dbm1) GAP (Chen et al. 1996), which interacts physically with Cdc42 (and more weakly with Rho1) (Stevenson et al. 1995). These observations suggest that Bem2, like Cdc42, may serve to link proteins involved in bud site selection to those involved in bud emergence.

Results

Suppression of the bem2-101 *mutation by increased dosage of* GIC1 *or its homolog* GIC2

To identify gene products that function with the Bem2 Rho-type GAP in the regulation of cellular morphogenesis, we isolated yeast genes that in high copy number could suppress the temperature-sensitive (Ts^-) growth defect of *bem2-101* mutant cells (see Materials and Methods). One such gene, which we named *GIC1* (GTPase-interacting component 1, see below), will be the subject of this report. A high copy number *GIC1* plasmid could suppress the Ts^- phenotype of *bem2-101* and *bem2* null mutant cells at 35 and 33°C, respectively (data not shown). Furthermore, this plasmid could suppress weakly the randomized bud site selection defect of *bem2-101* cells at 26°C (reducing the fraction of cells with randomized bud site selection pattern from ~41% to ~30%). Subcloning and partial sequence analysis revealed that *GIC1* is allelic to the hypothetical open reading frame (ORF) *YHR061c*. *GIC1* potentially encodes a protein of 314 residues, with a predicted molecular mass of 35 kD (Fig. 1A).

A search of the compiled databases at the National Center for Biotechnology Information (NCBI) revealed that the Gic1 protein is related in sequence to the putative gene product of the hypothetical yeast ORF *YDR309c*, which we have named *GIC2*. The Gic2 protein is predicted to contain 383 residues, with a molecular mass of 43 kD (Fig. 1A). Over the entire length of the protein, Gic1 displays 39% identity and 54% similarity to Gic2. Gic1 and Gic2 are not significantly homologous to other known proteins. Northern blot analysis revealed that *GIC1* as well as *GIC2* are expressed at similar levels in haploid (**a** or α) and diploid (**a**/α) cells (data not shown). A high copy number *GIC2* plasmid failed to suppress the Ts^- growth defect of *bem2-101* mutant cells, although it, like a *GIC1* plasmid, could suppress weakly the bud site selection defect of *bem2-101* cells at 26°C (reducing the fraction of cells with randomized bud site selection pattern from ~41% to ~32%). Thus, Gic1 and Gic2 have related, but perhaps not identical, functions in vivo.

Gic1, Gic2, and Bem2 together are essential for cell viability

To determine the importance of Gic1 and Gic2 for the normal growth of yeast cells, we examined the growth properties of cells lacking Gic1 and/or Gic2. Tetrad analysis of diploid yeast strains (CBY1830-51-1 or CBY1830-51-2) that are heterozygous for the *gic1* null (*gic1-Δ1::LEU2*) and the *gic2* null (*gic2-1::HIS3* or *gic2-Δ2::TRP1*) mutations (see Materials and Methods) revealed that haploid *gic1* and *gic2* mutant cells are viable on YEPD-rich medium at temperatures ranging from 13 to 37°C, and *gic2* cells have a reduced growth rate at 37°C. Furthermore, haploid *gic1 gic2* double mutant cells have normal growth rates at 26°C but are inviable at ⩾33°C (Fig. 2A). The Ts^- phenotype of *gic1 gic2* cells, unlike that of *bem2* cells, could not be rescued by the presence of an osmotic stabilizer (e.g., 1 M sorbitol; data not shown).

Further genetic analyses showed that the *gic1*, but not the *gic2*, mutation exacerbates slightly the Ts^- phenotype caused by the *bem2* null mutation, and that *gic1 gic2 bem2* triple mutant cells are extremely slow growing at 26°C, the permissive growth temperature for *gic1 gic2* double mutant and *bem2* single mutant cells (Fig. 2B). This synthetic relationship between *gic1*, *gic2*, and *bem2* mutations is consistent with the observed sup-

A

```
Gic1     2 TEGKRLQQMELPQMKSIWIDEDQEMEKLYGFQVRQRFMNGPSTDSDEDAD 51
           ....  : |:||||:|||:|||:| ||||:|. |.||.:        |.:
Gic2     6 ITNTGNETMNLPQMRSIWLDEDEEAEKLYGLQA.QQFMGS-------DDE 47

Gic1    52 EDLGIVLVDSKKLALPNKNNIKLPPL-----PNYMTINPNINSNHK.... 92
           |:|||.:::|.| .|.||.||.|||      |.:   ..| ||...
Gic2    48 ENLGITFINSDKPVLSNKKNIELPPLSPNSHPSCHHRRSNSNSAKSKESS 97

Gic1    93 ------SLTNKKKNPLGM.FKKKDLLSRRHGSAKTAKQSSISTPFDFHHI 135
                 . ||.|| || : : ||.||    |.... :..:|||||||:||
Gic2    98 SSSSSANKTNHKKVFLKLNLLKKKLL----GAQPDIRGKGISTPFDFQHI 143

Gic1   136 SHANGKR--EDNPLR--------------SHEEKHDVESLVKF------- 162
           |||:.:.  :|:.|:              | ..|:| .|| |
Gic2   144 SHADTRNGFQDEQLQEPSSLSTEIKDDYTSSSSKRDSKSLNKAFVTERIP 193

Gic1   163 --------------TSLAPQPRPDSNVSSKYSNVVMND----SSRIVSS 193
                         ||  . :|. | .||.||. . .:    .:|:||.
Gic2   194 ANRESKLISRSHENKTSRLSVARSISVTSSNYSKNTQGNNHSINGRVVST 243

Gic1   194 STIATTMDSHHDGNETNNTPN-----GNKQLDSPTDLEMTLEDLRNYTFP 238
           ||:||.: .. ..... .|     |::  :|... | .|: |:||.||
Gic2   244 STMATSIFEYSPNASPKQFKNKSHALGHRYTNSTDSSESSLDFLKNYNFP 293

Gic1   239 SVLGDSVSEKTNPSSPSVSSFSGKFK--------------------PREL 268
           .:|:|..  .  |.|.. |.:.: :.                    |:
Gic2   294 TLLEDKPILDFLPRSQRSSAYRSLLETPNSNKDSAKAFFPSRQSPLPKRR 343

Gic1   269 SALHTPELGNCFNVDQSLNSPGNRISVDDVLKFYYQCSETST 310
           ..: ||. .. |. .:|  ...:| |.|||  : | ..  |
Gic2   344 NSIATPSPQSKFSYSDS--PVNHRKSFDDVLYSFNQLEPLQT 383
```

B

ACK	(human)	**ISQPLQNSFIHTGH**
MLK3	(human)	**ISMPLD--FKHRIT**
MIHCK	(Dictyostelium)	VGS**P**FN--VK**H**NI**H**
α-PAK	(rat)	**ISLPSD--FEHTIH**
Ste20	(yeast)	**IST**PYN--AK**HIHH**
Cla4	(yeast)	**VSSP**TN--**FTHKVH**
Skm1	(yeast)	**VSSP**TN--**FTHKVH**
WASP	(human)	**IGAPSG--FKHVSH**
Gic2	(yeast)	**IST**PFD--**FQHISH**
Gic1	(yeast)	**IST**PFD--**F**HHI**SH**
Gic1-2		**IST**PFD--**F**HAI**SA**
Gic1-3		AAT**P**FD--**F**HAI**SA**

Figure 1. (*A*) Comparison of the predicted sequences of Gic1 (GenBank accession no. U00061) and Gic2 (GenBank accession no. U28374). Gaps introduced for alignment purposes (dashes) as well as sequence identity (vertical lines) and similarity (periods and colons) are indicated. The CRIB motif present in each protein is underlined. (*B*) Sequence comparison of the CRIB motifs present in ACK (GenBank accession no. L13738), MLK3 (GenBank accession no. L32976), MIHCK (GenBank accession no. U67716), α-PAK (GenBank accession no. U23443), Ste20 (GenBank accession no. L04655), Cla4 (GenBank accession no. X82499), Skm1 (GenBank accession no. X69322), WASP (GenBank accession no. U12707), Gic1, and Gic2. Sequences of the modified CRIB motif in mutant proteins Gic1-2 and Gic1-3 are also shown.

pression of the *bem2-101* mutation by increased dosage of *GIC1* and *GIC2,* and it indicated that Gic1, Gic2, and Bem2 together perform a function that is essential for yeast cell growth. We also examined the effect of increasing *BEM2* dosage in *gic1 gic2* mutant cells. Our results showed that a high copy number *BEM2* plasmid cannot suppress the Ts$^-$ phenotype of *gic1 gic2* cells (Fig. 3A). Interestingly, a low copy number *SSD1-v1* plasmid, which can suppress *bem2* mutations (Kim et al. 1994), could suppress the Ts$^-$ phenotype of *gic1 gic2* cells. *SSD1* is a polymorphic gene of unknown function (Sutton et al. 1991). Different laboratory yeast strains contain either the *SSD1-v1* or the *ssd1-d2* allele. The yeast strains used in this study presumably contained the *ssd1-d2* allele.

Gic1 and Gic2 together are required for proper bud site selection, bud emergence, and mitotic spindle orientation and positioning

To investigate whether Gic1 and Gic2, like Bem2, play important roles in cellular morphogenesis, we examined in greater detail the phenotype of haploid *gic1, gic2,* and *gic1 gic2* mutant cells. At 26°C, haploid *gic1* and *gic2* single mutant cells had normal cell shape, budding pattern, mating efficiency, and actin cytoskeleton that was polarized (data not shown). Cells of **a** mating type formed mating projections in response to α-factor with wild-type efficiency (≥90% of cells after 2 hr). After a 4-hr incubation at 37°C, *gic1* and *gic2* mutant cells remained normal in shape and size, and they exhibited normal actin organization and budding pattern (data not shown).

In contrast, haploid *gic1 gic2* double mutant cells were heterogeneous in shape and size at 26°C, with many (≤30%) cells being rounder and somewhat enlarged (Fig. 4d). These cells showed a moderate randomization of bud site selection, as indicated by an increase in the fraction of cells (~23%) that had a nonaxial budding pattern (Fig. 4f). The severity of this bud site selection defect was somewhat dependent on the genetic background of the

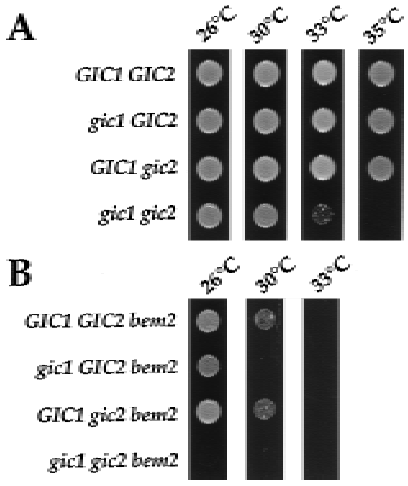

Figure 2. Synthetic growth phenotype caused by combinations of *gic1, gic2,* and *bem2* mutations. Suspensions of yeast cells were spotted on YEPD plates and allowed to grow at the indicated temperatures for 2 days. The yeast strains used were (*A*) CCY311-17A (*GIC1 GIC2*), CCY1033-11B (*gic1-Δ1::LEU2 GIC2*), CCY1033-5A (*GIC1 gic2-1::HIS3*), and CCY1033-5D (*gic1-Δ1::LEU2 gic2-1::HIS3*); and (*B*) CCY1030-11B (*GIC1 GIC2 bem2-Δ110::TRP1*), CCY1030-10C (*gic1-Δ1::LEU2 GIC2 bem2-Δ110::TRP1*), CCY1030-6D (*GIC1 gic2-1::HIS3 bem2-Δ110::TRP1*), and CCY1030-28D (*gic1-Δ1::LEU2 gic2-1::HIS3 bem2-Δ110::TRP1*).

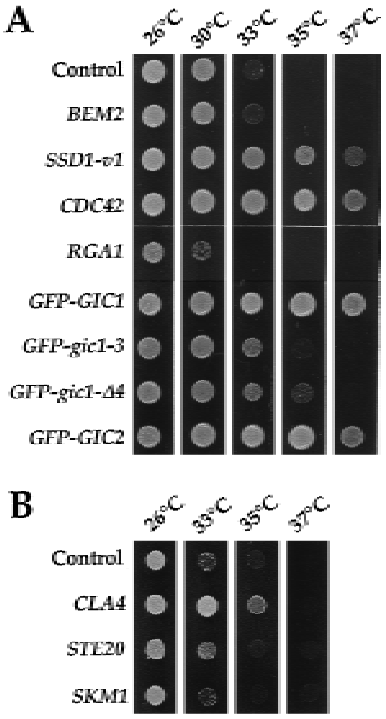

Figure 3. Ts⁻ growth phenotype of a *gic1 gic2* mutant carrying different plasmids. Suspensions of *gic1-Δ1::LEU2 gic2-1::HIS3* (CCY1024-19C) mutant cells carrying different plasmids were spotted on YEPD (*A*) or supplemented SD lacking uracil (*B*) plates and allowed to grow at the indicated temperatures for 2 days. The plasmids used were high copy number control plasmid pSM217, *BEM2*-containing high copy number plasmid pCC251, *SSD1-v1*-containing low copy number plasmid pCC75, *CDC42*-containing high copy number plasmid YEpU-CDC42, *RGA1*-containing high copy number plasmid pCC693, *GFP–GIC1*-containing low copy number plasmid pCC995, *GFP–gic1-3*-containing low copy number plasmid pCC1051-1, *GFP–gic1-Δ4*-containing low copy number plasmid pCC1067-1, *GFP–GIC2*-containing low copy number plasmid pCC1065-1, *CLA4*-containing high copy number plasmid pCC1079, low copy number plasmid pVTU–STE20 that carries *STE20* under the control of the *ADH1* promoter, and *SKM1*-containing high copy number plasmid YEp352-SKM1.

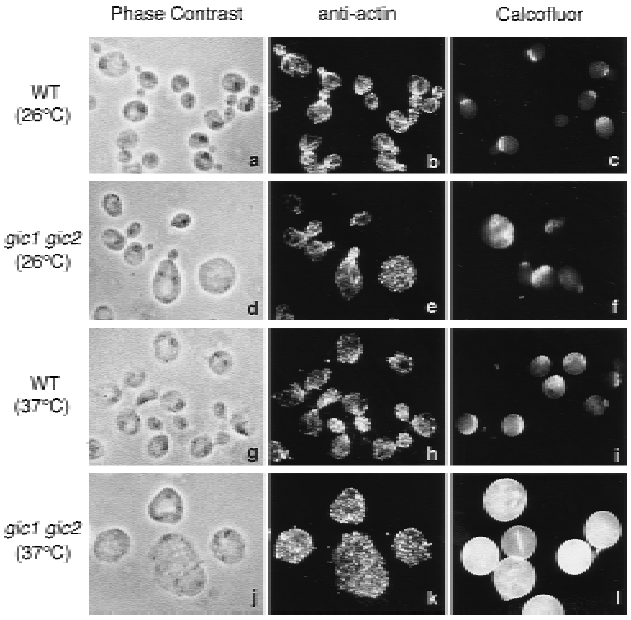

Figure 4. Cytological examination of wild-type and *gic1 gic2* mutant cells. Wild-type (CCY441-52D) (*a–c* and *g–i*) and *gic1 gic2* (CCY1024-19C) (*d–f* and *j–l*) haploid cells grown at 26°C or at 37°C for 4 hr were fixed and stained with Calcofluor or anti-actin antibodies. The phase and anti-actin staining images were obtained from the same cells. All cells are shown at the same magnification.

yeast strains tested (data not shown). Many of the larger *gic1 gic2* double mutant cells also exhibited delocalized cell surface growth, as indicated by the presence of diffused chitin staining, which was not restricted to bud scars (Fig. 4f). The organization of the actin cytoskeleton was also somewhat perturbed in many of the larger *gic1 gic2* mutant cells, with the high concentration of cortical actin patches normally found at one end of some unbudded wild-type cells either missing or reduced (Fig. 4e). After a 2-hr exposure to α-factor, ~98% of *gic1 gic2* cells of **a** mating type became arrested as unbudded cells, but only 60–70% of these cells formed mating projections, suggesting that the round and enlarged cells are defective in mating projection formation. However, *gic1 gic2* mutant cells mated with normal efficiency with both wild-type and *gic1 gic2* mutant cells (data not shown).

DAPI staining showed that about one third of the larger *gic1 gic2* cells were multinucleate (Fig. 5j–l). Anti-tubulin staining revealed the presence of mitotic spindles in some enlarged, unbudded cells, suggesting

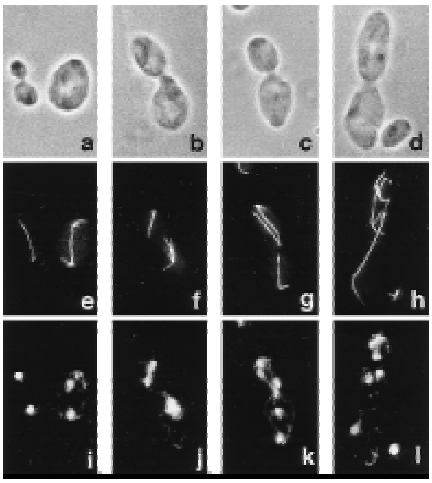

Figure 5. Abnormal mitotic spindle behavior of *gic1 gic2* mutant cells. *gic1 gic2* (CCY1024-19C) haploid cells grown at 26°C were fixed and stained with DAPI or anti-tubulin antibodies. Phase (*a–d*), anti-tubulin staining (*e–h*), and DAPI-staining (*i–l*) images are shown.

that these cells are defective in bud emergence even at 26°C (Fig. 5e). Mitotic spindles were misoriented in a small number of the budded cells (Fig. 5f,h). More frequently, the positioning of the spindles appeared abnormal, with spindles that lay entirely or mostly within the mother or the bud of large budded cells (Fig. 5f–h), indicating that nuclear migration occurred, but that this process might not be regulated properly. In a small fraction of cells with two or more mitotic spindles, the lengths of the spindles differed greatly (Fig. 5h), thus suggesting that the timing for the onset of anaphase or the rate of spindle elongation is not coordinated between the multiple spindles within a single cell. We do not know whether this property is unique to *gic1 gic2* cells, or whether it is common to other multinucleate yeast cells. Because spindle defects were seen mostly in *gic1 gic2* cells that were enlarged or round, they likely occurred as a consequence of the morphological defects observed in these cells. However, we cannot rule out the possibility that Gic1 and Gic2 play a more direct role in regulating spindle behavior. After a 4-hr incubation at 37°C, ~80% of *gic1 gic2* double mutant cells became arrested as unbudded cells that were mostly round and enlarged (see Fig. 4j). The actin cytoskeleton in these cells was no longer polarized (Fig. 4k), and they exhibited delocalized cell surface growth and chitin deposition (Fig. 4l). Thus, Gic1 and Gic2 play important roles in polarized growth and spindle behavior, especially at elevated temperatures.

Gic1 and Gic2 can associate with the Cdc42 GTPase

The phenotypes of *gic1 gic2* mutant cells are similar in many respects to those exhibited by *bem2* and, interestingly, *cdc42* mutant cells (Adams and Pringle 1984; Adams et al. 1990; Bender and Pringle 1991; Chan and Bostein 1993; Kim et al. 1994; Peterson et al. 1994; Wang and Brescher 1995). Examination of the Gic1 and Gic2 sequences revealed that each protein contains a Cdc42/Rac-interactive binding (CRIB) motif (see Fig. 1A,B), which is present in a number of proteins that bind the GTP-bound form of the Rho-type Cdc42 and Rac GTPases (Burbelo et al. 1995). We used the two-hybrid assay (Finey and Brent 1994) to investigate whether Gic1 or Gic2 physically interacts in vivo with known yeast Rho-type GTPases, specifically Cdc42, Rho1, Rho2, Rho3, and Rho4 (Simon et al. 1995). Our results showed that fusion proteins with the B42 transactivation domain (AD) fused to full-length Gic1 or Gic2 (Gyuris et al. 1993) interact specifically with LexA–Cdc42 (which was nonprenylated as a result of the *C188S* mutation) but not the other GTPase fusion proteins tested (Fig. 6). This interaction required an intact effector domain of LexA–Cdc42, which was altered by the *T35A* mutation (Ziman et al. 1991). Interaction was specific for the GTP-bound form of LexA–Cdc42 (*G12V* or *Q61L*); no interaction was detected with mutant LexA–Cdc42 (*D118A*) that was trapped in the GDP-bound state.

To find out whether the CRIB motif present on Gic1 is required for the association between Gic1 and Cdc42, we

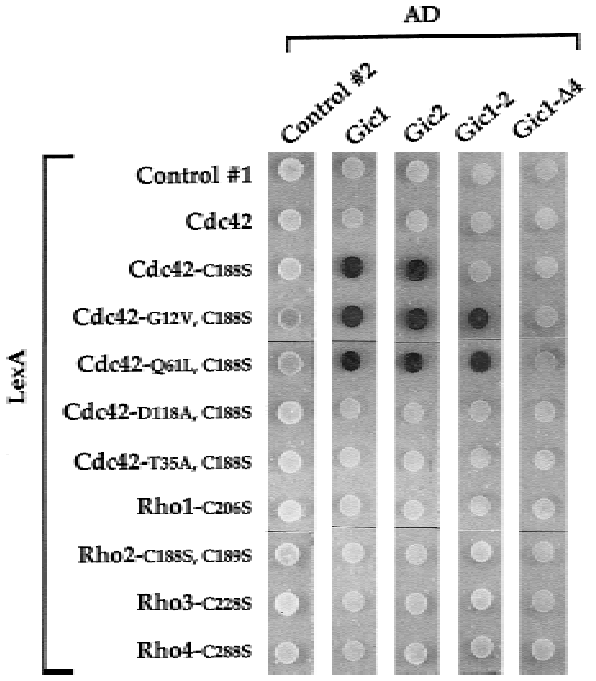

Figure 6. CRIB motif-dependent interaction of Gic1 and Gic2 with GTP-bound Cdc42 in the two-hybrid assay. Suspensions of diploid yeast cells (EGY48 [pSH18-34] × RFY206) containing combinations of the following plasmids were spotted on SGal/Raf/XGal plates and were allowed to grow at 30°C for 4 days. Blue color (seen here as dark color) indicates a specific interaction in the two-hybrid assay. The plasmids used were pEG202 (Control #1), pEG202–CDC42 (Cdc42), pEG202–CDC42^{C188S} (Cdc42–C188S), pEG202–CDC42^{G12V,C188S} (Cdc42–G12V, C188S), pEG202–CDC42^{Q61L,C188S} (Cdc42–Q61L, C188S), pEG202–CDC42^{D118A,C188S} (Cdc42–D118A, C188S), pCC1081-2 (Cdc42–T35A, C188S), pEG202–RHO1^{C206S} (Rho1–C206S), pEG202–RHO2^{C188S,C189S} (Rho2–C188S, C189S), pEG202–RHO3^{C228S} (Rho3–C228S), pEG202–RHO4^{C288S} (Rho4–C288S), pJG4-5 (Control #2), pCC984 (Gic1), pCC985 (Gic2), pCC1044-1 (Gic1-2), and pCC1066-1 (Gic1-Δ4).

generated mutant AD–Gic1 that had two (AD–Gic1-2) or four (AD–Gic1-3) of the conserved residues within the CRIB motif substituted by alanine (see Fig. 1B), as well as mutant AD–Gic1 that lacked the 12 residues that define the CRIB motif (AD–Gic1-Δ4). Interaction was still detected, although at a reduced level, between AD–Gic1-2 and GTP-bound forms of LexA–Cdc42. No interaction was detected between AD–Gic1-3 or AD–Gic1-Δ4 and any form of LexA–Cdc42 tested (Fig. 6; data not shown). These results indicated that the interaction of Gic1 with Cdc42 requires its CRIB motif, and that at least one of the two conserved histidine residues of the CRIB motif in Gic1 is important, although not absolutely essential, for the function of this motif.

Genetic interactions between GIC1, GIC2, *and* CDC42

To find out more about the functional relationship between Gic1, Gic2, and Cdc42, we examined possible ge-

netic interactions between *GIC1, GIC2, CDC42, CDC24,* and *RGA1*. *CDC24* encodes the GDP dissociation stimulator (and thus positive regulator) for Cdc42 (Zheng et al. 1994), whereas *RGA1* encodes a putative GAP that associates with Cdc42 and functions as its negative regulator in vivo (Stevenson et al. 1995; Chen et al. 1996). Our results showed that the *gic2* mutation exacerbates the Ts$^-$ phenotype caused by the *cdc42-1* and *cdc24-2* mutations (Fig. 7). Furthermore, *gic1 gic2 cdc42-1* triple mutant cells were extremely slow growing at 26°C, the permissive growth temperature for *cdc42-1* and *gic1 gic2* mutant cells (Figs. 2 and 7), and *gic1 gic2 cdc24-2* triple mutant cells were slow growing at 30°C, the permissive growth temperature for *cdc24-2* and *gic1 gic2* mutant cells (Figs. 2 and 7). In addition, a high copy number *CDC42* plasmid, but not a similar *CDC24* plasmid, could complement the Ts$^-$ phenotype of *gic1 gic2* mutant cells at 37°C (see Fig. 3A; data not shown). This effect was specific to *CDC42,* as similar plasmids carrying *RHO1, RHO2, RHO3,* or *RHO4* could not complement *gic1 gic2* mutant cells (data not shown). In contrast, a high copy number *RGA1* plasmid exacerbated the Ts$^-$ phenotype of *gic1 gic2* mutant cells at 30°C (see Fig. 3A). These genetic results, together with the two-hybrid assay results described above, suggested that Gic1 and Gic2 play a positive role in the Cdc42 pathway through their interaction with Cdc42.

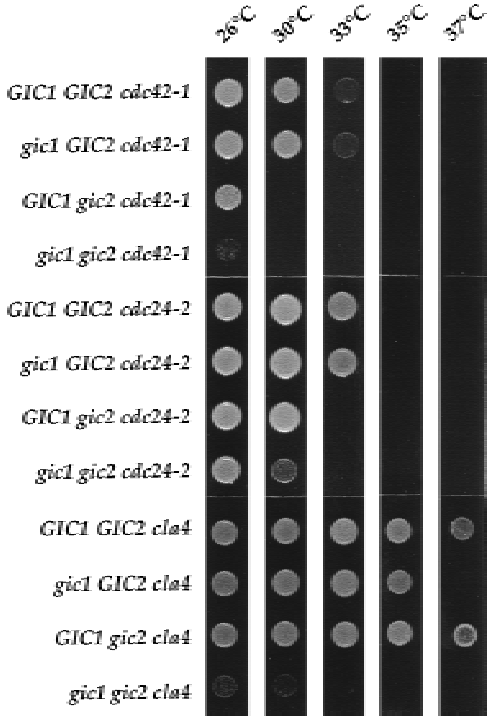

Figure 7. Exacerbation of the growth defect of *gic1, gic2,* and *gic1 gic2* cells by *cdc24, cdc42,* and *cla4* mutations. Suspensions of yeast cells were spotted on YEPD plates and allowed to grow at the indicated temperatures for 2 days. The yeast strains used were CCY896-8B (*GIC1 GIC2 cdc42-1*), CCY1027-24A (*gic1-Δ1::LEU2 GIC2 cdc42-1*), CCY1027-6A (*GIC1 gic2-1::HIS3 cdc42-1*), CCY1027-11D (*gic1-Δ1::LEU2 gic2-1::HIS3 cdc42-1*), CCY1032-16B (*GIC1 GIC2 cdc24-2*), CCY1032-6B (*gic1-Δ1::LEU2 GIC2 cdc24-2*), CCY1032-3A (*GIC1 gic2-1::HIS3 cdc24-2*), CCY1032-2B (*gic1-Δ1::LEU2 gic2-1::HIS3 cdc24-2*), CCY1056-6A (*GIC1 GIC2 cla4-Δ101::URA3*), CCY1055-16C (*gic1-Δ1::LEU2 GIC2 cla4-Δ101::URA3*), CCY1055-12B (*GIC1 gic2-1::HIS3 cla4-Δ101::URA3*), and CCY1055-4C (*gic1-Δ1::LEU2 gic2-1::HIS3 cla4-Δ101::URA3*).

Genetic interactions between GIC1, GIC2, *and* CLA4

Because increased dosage of *CDC42* could suppress the loss of *GIC1* and *GIC2,* Cdc42 may act downstream of Gic1 and Gic2. Alternatively, Gic1 and Gic2 may act as downstream effectors of Cdc42, with some function of Gic1 and Gic2 shared by other effectors of Cdc42, perhaps Ste20 (Simon et al. 1995; Zhao et al. 1995), Cla4 (Cvrcková et al. 1995), or Skm1 (Martin et al. 1997). To explore this latter possibility, we examined the genetic relationship between *GIC1, GIC2, STE20, CLA4,* and *SKM1*. Our results showed that the *ste20* and *skm1* mutations did not significantly affect the growth phenotype of *gic1, gic2,* or *gic1 gic2* mutant cells (data not shown). In contrast, the *cla4* mutation often caused *gic1* mutant cells to be Ts$^-$ at 37°C, and *gic1 gic2 cla4* triple mutant cells were very slow growing at 26°C, the permissive growth temperature for *cla4* and *gic1 gic2* cells (Figs. 2 and 7). Furthermore, overexpression of *CLA4,* but not *STE20* or *SKM1,* could complement partially the Ts$^-$ phenotype of *gic1 gic2* mutant cells at 35°C (see Fig. 3B). These genetic results suggested that Gic1, Gic2, and Cla4 function together as effectors of Cdc42 and that together they perform functions essential for polarized cell growth.

Subcellular localization of Gic1

To determine the subcellular localization of Gic1 and Gic2, we generated fusion genes encoding the green fluorescent protein (GFP) fused to full-length Gic1 or Gic2 (Heim et al. 1995). The *GFP–GIC1* and *GFP–GIC2* fusion genes, which were under the control of the *ACT1* promoter, were functional, as a low copy number plasmid encoding GFP–Gic1 or GFP–Gic2 could complement the Ts$^-$ phenotype of *gic1 gic2* mutant cells at 37°C (see Fig. 3A). The fluorescence signal of GFP–Gic2-expressing cells was weaker. Thus, we have concentrated on the study of GFP–Gic1. This fusion protein was present throughout the cytoplasm of diploid cells that expressed this protein. Approximately 45% of these cells had additional GFP–Gic1 that was detected as one or more patches at the cell periphery (cortical) and ~13% had a narrow band of GFP–Gic1 at the mother-bud neck. In a minor fraction of these cells, GFP–Gic1 was also slightly enriched in the nucleus. The localization pattern of GFP–Gic1 likely reflects that of endogenous Gic1 because the fluorescence signal of GFP–Gic1 at cortical sites and at the mother-bud neck was stronger in *gic1* null mutant cells than in wild-type cells (data not

shown), suggesting that GFP–Gic1 competes with endogenous Gic1 for common binding sites.

In unbudded diploid cells, cortical GFP–Gic1 was detected mostly (~93%) as a single patch at one pole of the cell (Figs. 8a and 9, class a) and less frequently (~7%) as two patches (which sometimes differed in intensity) at both poles (Figs. 8b and 9, class b). In cells with small- to medium-sized buds, cortical GFP–Gic1 was detected almost exclusively as a single patch (which might be quite diffuse and in the shape of a crescent) at the tip of the bud (Figs. 8c–e and 9, classes d,e). These observations suggested that one of the two patches of GFP–Gic1 seen in some unbudded cells disappears before bud emergence, and that the remaining patch is located at the incipient bud site. In large-budded diploid cells, cortical GFP–Gic1 was most frequently detected as a patch at the tip of the bud (Figs. 8g,h,i,l,m and 9, classes k,l,n–p). Interestingly, many large budded cells, including those that had GFP–Gic1 at their bud tips, also had a patch of GFP–Gic1 that was most frequently located either at the tip of the mother (Figs. 8l,m and 9, classes n,o) or at the mother-side of the mother-bud neck (Figs. 8k,n and 9, classes p–r,t). Ninety-nine percent of such cells ($n = 100$) had fully separated chromatin masses (Fig. 8n,o), suggesting that this patch of GFP–Gic1 first appears during telophase or early G_1.

In some cells with medium- to large-sized buds, including those that had cortical GFP–Gic1, the fusion protein was also detected as a narrow band (or occasionally as two closely apposed bands) at the mother-bud neck (Figs. 8f,g,i,j,l and 9, classes e,f,l,m,o,r). Approximately 31% of these cells ($n = 100$) had unseparated chromatin masses, including some (~6%) that had the nucleus located away from the mother-bud neck. These observations suggested that GFP–Gic1 becomes localized to the mother-bud neck before the onset of anaphase and it persists at this site through telophase. The presence of large-budded cells with GFP–Gic1 at either (or both) pole as well as at the mother-bud neck (Fig. 9, classes l,o) suggested that these cells give rise after cytokinesis to unbudded cells with cortical GFP–Gic1 at both poles (Fig. 9, class b). Alternatively, in a bipolar budding diploid cell, GFP–Gic1 may localize to an incipient bud site that is located distal to the site of cytokinesis before the disappearance of GFP–Gic1 from this latter site.

Effect of bud site selection on Gic1 localization

The positions of cortical GFP–Gic1 in large-budded diploid cells suggested that they are located at sites used for budding by the progeny cells after cytokinesis, with one cell budding from either pole, and the other budding preferentially from the pole opposite the site of the previous cell division. Thus, we also examined the localization pattern of GFP–Gic1 in wild-type **a** haploid cells, which bud mostly from a site near the site of the previous cell division. As expected, GFP–Gic1 was restricted to only one pole of unbudded cells (Fig. 9, class a) and it was absent from the mother tip of large-budded haploid cells (Fig. 9, classes n,o). Furthermore, it was often present at cortical sites located adjacent to the mother-bud neck (Figs. 8p,q,r, and 9, classes g,p–u). However, this fusion protein was still present at the tip of some buds (Fig. 9, classes d,e,k,l,p). The observation that large-budded haploid cells with cortical GFP–Gic1 at both the bud tip and at other cortical sites were rarely seen suggested that

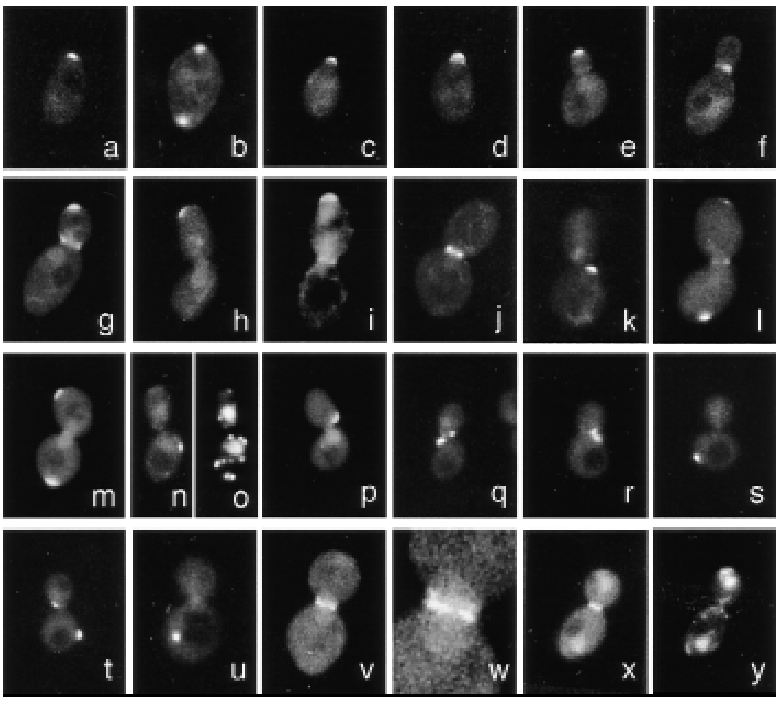

Figure 8. Subcellular localization of GFP–Gic1 and GFP–Gic1-Δ4. Subcellular localization of GFP–Gic1 (*a–n* and *p–u*), GFP–Gic1-Δ4 (*v–x*), and DNA (*o,y*) in wild-type diploid (DBY1830) (*a–o* and *v–y*), wild-type haploid (CCY766-9D) (*p–r*), and *bud5* haploid (CCY404-2D) (*s–u*) cells. The DAPI-stained images of DNA shown in *o* and *y* were obtained from the cells shown in *n* and *x*, respectively. (*w*) An enlarged view of the cell shown in *v*.

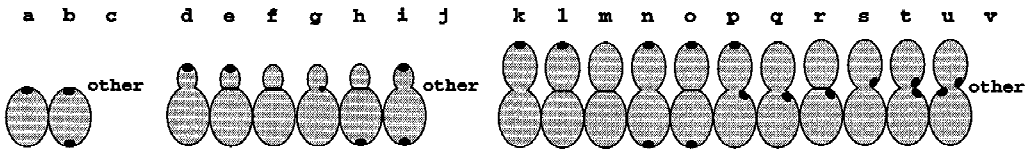

Yeast strain	GFP-fusion	a	b	c	d	e	f	g	h	i	j	k	l	m	n	o	p	q	r	s	t	u	v
W.T. diploid	Gic1	93	7	0	82	4	14	0	0	0	0	51	8	7	9	5	8	9	1	1	1	0	0
W.T. diploid	Gic1-Δ4	91	8	1	82	4	9	1	1	1	2	10	4	70	1	0	1	7	3	0	0	0	4
W.T. haploid	Gic1	100	0	0	73	2	17	8	0	0	0	33	1	30	0	0	1	16	0	10	3	5	1
bud3 haploid	Gic1	98	2	0	56	16	28	0	0	0	0	26	18	30	4	3	0	9	1	3	4	0	2

Figure 9. Summary of subcellular localization of GFP–Gic1 and GFP–Gic1-Δ4. Yeast cells carrying low copy number plasmids that encode GFP–Gic1 or GFP–Gic1-Δ4 were grown in supplemented SD lacking uracil (with selection for *URA3* present on the different plasmids) at ~24°C to a density of ~5×10^6 cells/ml. The localization of the GFP fusion protein was examined in cells at different stages of the cell cycle: Unbudded (*a–c*), small- to medium-budded (*d–j*), and large-budded (*k–v*). The length of the bud in medium-budded cells is less than half the length of the mother cell. For each sample, ≥300 cells that showed cortical or bud neck localization of GFP fusion protein were scored. The percentage of cells at each stage that showed the different localization patterns is shown. The nuclear localization of GFP fusion protein present in some cells is not shown. The yeast strains used were DBY1830 (wild-type diploid), CCY766-9D (wild-type haploid), and CCY1048-11A (*bud3* haploid). The plasmids used were pCC995 (GFP–Gic1) and pCC1067-1 (GFP–Gic1-Δ4).

GFP–Gic1 mostly disappears from the bud tip before it reappears during telophase or early G_1 (see above) at cortical sites that are used for budding after cytokinesis. We have also examined the localization of GFP–Gic1 in haploid **a** cells that had been exposed to mating pheromone. In such cells, GFP–Gic1 was found mostly in a single patch at or near the tip of mating projections (data not shown).

To confirm that the observed differences in the pattern of GFP–Gic1 localization in haploid and diploid cells was indeed attributable to differences in bud site selection (i.e., axial vs. bipolar) and not attributable to differences in cell type (i.e., **a** vs. **a**/α) or ploidy, we examined the localization pattern of GFP–Gic1 in **a** *bud3* and *bud5* mutant haploid cells, which have a bipolar (i.e., like wild-type **a**/α diploid cells) and a randomized bud site selection pattern, respectively (Chant and Herskowitz 1991; Chant et al. 1991, 1995). Our results showed that the localization pattern of GFP–Gic1 in *bud3* haploid cells was similar to that observed in wild-type diploid cells (Fig. 9). The observation that GFP–Gic1 was detected at cortical sites located on the bud-side of the mother-bud neck at a slightly higher frequency in *bud3* haploid than in wild-type diploid cells (Fig. 9, classes s,t) was probably attributable to the fact that, although diploid daughter cells are biased toward budding from the pole opposite the site of the previous cell division, the strength of this bias varies from strain to strain (Chant and Pringle 1995). In *bud5* haploid cells, which often bud from the lateral side and not from the poles of the ellipsoidal cell, cortical GFP–Gic1 was detected on the side of ~16% of large-budded cells (Fig. 8s,t). These results indicated that GFP–Gic1 localizes to the incipient bud site of unbudded cells, to the tip of budded cells where it persists for part of the period of bud growth, and to the mother-bud neck of cells with medium- to large-size buds. In addition, it localizes in large-budded cells to sites that are used for budding by the two progeny cells in the subsequent cell cycle.

Effect of CRIB motif mutation on Gic1 localization

To find out whether the localization of GFP–Gic1 is dependent on its association with Cdc42, we examined the localization of GFP–Gic1-Δ4, which lacks the 12 residues that define the CRIB motif of Gic1 (see Fig. 1B). This protein was expected not to bind Cdc42 in vivo because AD–Gic1-Δ4 did not associate with LexA–Cdc42 in the two-hybrid assay (see Fig. 6). Consistent with this prediction, *GFP–gic1-Δ4,* unlike *GFP–GIC1,* was unable to complement the Ts^- phenotype of *gic1 gic2* mutant cells at 37°C (see Fig. 3A), although GFP–Gic1-Δ4 was present in somewhat higher abundance than GFP–Gic1 (data not shown).

Our cytological studies revealed interesting differences between the localization patterns of GFP–Gic1 and GFP–Gic1-Δ4 in wild-type diploid cells. First, the abundance of GFP–Gic1-Δ4 present at the bud neck was slightly reduced, but a slightly increased fraction (~16%) of cells that expressed GFP–Gic1-Δ4 had this protein localized to the bud neck (Fig. 9,e,f,h,l,m,o,r). [The apparent large increase in the fraction of large-budded cells with GFP–Gic1-Δ4 at the bud neck was attributable to the decrease in the fraction of cells with this protein at cortical sites (see below).] Second, an increased fraction (~10%) of large-budded cells that had GFP–Gic1-Δ4 at the bud neck contained a doublet (instead of a singlet) of bands at this site (Fig. 8v,w). Third, although GFP–Gic1-Δ4 was still present at cortical sites, its abundance was reduced. This reduction might account at least partly for

the smaller fraction (~27%) of GFP–Gic1-Δ4-expressing cells that had this fusion protein detected at cortical sites as well as the increased cytoplasmic fluorescence signal (Fig. 8v,x). Fourth, the abundance of GFP–Gic1-Δ4 present in the nucleus was greatly increased (Fig. 8x,y), and ~18% of GFP–Gic1-Δ4-expressing cells had this fusion protein detected in the nucleus. Similar results were obtained for the localization of GFP–Gic1-3 (see Fig. 1B) in wild-type cells or GFP–Gic1-Δ4 in *gic1*- or *gic1 gic2*-null mutant cells (data not shown), thus arguing that the localization pattern of GFP–Gic1-Δ4 was not attributable to its possible misfolding caused by the 12-amino acid deletion or to its oligomerization with wild-type Gic1 or Gic2.

These results indicated that (1) the localization of GFP–Gic1 to the bud neck is mostly independent of its ability to associate with Cdc42, but the exact pattern of localization at this site is affected by this function of GFP–Gic1; and (2) the ability of GFP–Gic1 to associate with Cdc42 is important, but not absolutely essential, for its localization to cortical sites. These results also suggested that GFP–Gic1-Δ4 may not be totally nonfunctional. *GFP–gic1-Δ4* could complement partially the Ts^- phenotype of *gic1 gic2* mutant cells at 35°C and the cell size and shape control defect of these cells at 26°C (see Fig. 3A; data not shown).

Discussion

Gic1 and Gic2 as putative effectors of Cdc42

In this report, we describe *GIC1,* a novel gene identified as a dosage-dependent suppressor of *bem2,* and its structural and functional homolog *GIC2* (Fig. 1). Gic1 and Gic2 together are required for cell viability at elevated temperatures (Fig. 2). In the two-hybrid assay, Gic1 and Gic2 associate with the GTP-bound but not the GDP-bound form of Cdc42 (Fig. 6). This association is dependent on the effector domain of Cdc42 and the CRIB motif of Gic1 (and probably Gic2). Because the Ts^- phenotype of *gic1 gic2* mutant cells is exacerbated by perturbations (e.g., the *cdc42-1* and *cdc24-2* mutations, or increased dosage of *RGA1*) that reduce Cdc42 function (Figs. 3A and 7), Gic1 and Gic2 must play a positive role in the Cdc42 signal transduction pathway, most probably as effectors of Cdc42, although we cannot rule out the possibility that they may also function as positive regulators of Cdc42. Consistent with the observed genetic and physical interactions, *gic1 gic2* mutant cells, like *cdc42* mutant cells, are defective in bud site selection, organization of the actin cytoskeleton, polarized cell surface growth, bud emergence, and mating projection formation (Fig. 4). If Gic1 and Gic2 are effectors of Cdc42, their functions are probably shared by at least one other effector protein. This is because *gic1 gic2* null mutant cells are viable at 26°C, whereas *cdc42* null mutant cells are inviable at this temperature (Johnson and Pringle 1990). Furthermore, the Ts^- phenotype of *gic1 gic2* mutant cells can be suppressed by an increase in the dosage of *CDC42* (Fig. 3A). This other effector protein may be the Cla4 protein kinase, as *gic1 gic2 cla4* null mutant cells are very slow growing at 26°C (Fig. 7), and an increase in the dosage of *CLA4* can suppress partially the Ts^- phenotype of *gic1 gic2* cells (Fig. 3B). Cla4, like Gic1 and Gic2, associates with the GTP-bound form of Cdc42, and it is known to be required for efficient cytokinesis and proper control of polarized cell surface growth (Benton et al. 1993; Cvrcková et al. 1995).

The subcellular localization and function of Gic1

Polarized vegetative growth of yeast cells is thought to involve cortical positional signals that recruit polarity establishment proteins such as Cdc42 to incipient bud sites, where such proteins function in the process of bud emergence (for review, see Roemer et al. 1996). In haploid cells that bud axially, the positional signal is thought to be located transiently at the site of cytokinesis, where it serves after cell division as a template for the assembly of an adjacent positional signal that is used for budding. A number of proteins have been localized to the site of cytokinesis, and they may function as part of the axial budding positional signal (for review, see Roemer et al. 1996). In diploid cells that bud bipolarly, the positional signal is thought to be located at both poles of an unbudded cell. The nature of the bipolar budding positional signal is less understood because until recently no protein had been localized to the pole distal to the site of cytokinesis in mother cells.

Our localization study of GFP–Gic1 (and presumably Gic1) has provided important insights into the problem of bud site selection and its connection to bud emergence (Figs. 8 and 9). In large-budded cells that have completed chromosome segregation, GFP–Gic1 can be detected at cortical sites that are located at the poles or adjacent to the mother-bud neck. Examination of the location of these cortical sites in cells with different bud site selection patterns suggests that they are located at incipient bud sites for the progeny cells. Our preliminary results with time-lapse microscopy are consistent with this assignment (G. Chen and C. Chan, unpubl.). These observations show that bud site selection does not occur after cell division as proposed previously (for review, see Roemer et al. 1996). Instead, it may occur during telophase of the previous cell cycle or during early G_1 just before cytokinesis and cell separation. To our knowledge, the appearance of GFP–Gic1 at the incipient bud site precedes that of all but one known protein. Aip3 (Bud6), which is needed for the bipolar budding pattern (Zahner et al. 1996), has also been localized to incipient bud sites present on the mother-side of large-budded cells (Amberg et al. 1997). However, Aip3 differs from GFP–Gic1 in that it is not localized to incipient bud sites that are present on the bud side of large-budded cells. In spite of the strategic localization of GFP–Gic1 to incipient bud sites in both axial and bipolar budding cells, *gic1 gic2* mutant cells have relatively moderate bud site selection defects. This suggests that in the absence of Gic1 and Gic2, other proteins that constitute the axial and

bipolar specific positional signals can still be localized properly.

After cytokinesis, GFP–Gic1 appears to remain at the incipient bud site of unbudded cells, where it presumably interacts with Cdc42 to carry out the process of bud emergence. GFP–Gic1 persists at the bud tip of small- to large-budded cells. Cortical actin structures are known to be concentrated at incipient bud sites of unbudded cells and at the tip of small-budded cells (Kilmartin and Adams 1984). Because the concentration of cortical actin structures at incipient bud sites becomes less pronounced in unbudded *gic1 gic2* mutant cells that are enlarged, Gic1 (and Gic2) may play a role in organizing the cortical actin structures at this location, thus directly controlling bud emergence and growth. Interestingly, GFP–Gic1 seems to disappear from the bud tip in large-budded cells. The exact timing of this disappearance is not known, but it probably occurs before or during telophase, when it relocalizes to incipient bud sites (including those located at the bud tip). The activation and inactivation of the Cdc28/mitotic cyclin complex during G_2/M phase is known to control the redistribution of cortical actin structures from the bud tip to the entire bud and then to the bud neck (Lew and Reed 1993). It remains to be determined whether the disappearance of GFP–Gic1 from the bud tip and its reappearance at incipient bud sites is similarly controlled.

GFP–Gic1 is also present in a band (or two closely apposed bands) that spans the mother-bud neck of cells with medium- to large-sized buds. Upon cytokinesis, this band may give rise to a patch of GFP–Gic1 that probably disappears before the next round of budding. The functional role of Gic1 at the mother-bud neck is unknown. The localization of GFP–Gic1 at this site is not required for its localization to adjacent incipient bud sites, and *gic1 gic2* cells do not have noticeable cytokinesis defects. However, the *gic1 gic2* mutations confer an extremely slow growth phenotype when combined with the *cla4* mutation, which causes defects in cytokinesis (Benton et al. 1993; Cvrcková et al. 1995), thus suggesting that Gic1 and Gic2 may play a redundant and normally dispensable role in cytokinesis. Consistent with this idea, *gic1 gic2 cla4* mutant cells have a more severe cytokinesis defect than that of *cla4* cells (G. Chen and C. Chan, unpubl.).

Cdc42 is present at the incipient bud site of unbudded cells, at the bud tip of budded cells, and at the mother-bud neck at the time of cytokinesis (Ziman et al. 1993; E. Bi, pers. comm.). In spite of the partial overlap in the localization pattern of GFP–Gic1 and Cdc42, the localization of GFP–Gic1 to the sites described above is largely independent of its ability to associate with Cdc42. Mutant GFP–Gic1 that cannot associate with Cdc42 is still found in the cortical patches, albeit at reduced levels, suggesting that Cdc42 is not absolutely required to direct GFP–Gic1 to these sites but instead may help to stabilize it at these locations. In this context, it is important to note that Cdc42 is not found at all cortical sites in which GFP–Gic1 has been detected (e.g., at incipient bud sites in large-budded cells). In addition, mutant GFP–Gic1 that cannot bind Cdc42 still localizes to the mother-bud neck. This observation is not surprising because GFP–Gic1 is found at this site relatively early in the cell cycle (i.e., before onset of anaphase), whereas Cdc42 only localizes to this site at around the time of cytokinesis (Ziman et al. 1993; E. Bi, pers. comm.). Although mutant GFP–Gic1 that cannot associate with Cdc42 appears to be properly localized in many cells, it is only partially functional, as it can complement only partially the Ts^- phenotype of *gic1 gic2* mutant cells, indicating that the association between Cdc42 and Gic1 is functionally important.

In addition to cortical sites and the mother-bud neck, GFP–Gic1 is also somewhat concentrated in the nucleus. This is especially obvious for mutant forms of GFP–Gic1 that cannot associate with Cdc42. Although the function of GFP–Gic1 (and presumably Gic1) in the nucleus is unknown, this observation raises the intriguing possibility that Gic1 may shuttle between the nucleus and the cell cortex, where Cdc42 is concentrated, thus transducing signals between these sites. WASP, a human CRIB motif-containing protein that binds Cdc42, has also been detected both in the cytoplasm and within the nucleus (Symons et al. 1996).

Relationship between Bem2 and Cdc42

The carboxy-terminal 201-residue segment of Bem2 functions in vitro as a GAP for the Rho1 but not the Cdc42 Rho-type GTPase (Zheng et al. 1993, 1994; Peterson et al. 1994), thus suggesting that Bem2 functions in vivo as a regulator of Rho1. However, the Sac7 protein has been shown recently to function in vivo as a GAP for Rho1 (Schmidt et al. 1997). The mutant phenotype caused by inactivation of Tor2, a positive regulator of Rho1, can be suppressed by the *sac7* mutation, but not by the *bem2* mutation; and the phenotype of *sac7* mutant cells can be suppressed by increased dosage of the *SAC7* homolog *BAG7,* but not *BEM2* (Schmidt et al. 1997). Furthermore, the phenotype of *bem2* mutant cells is suppressed partially, rather than exacerbated, by the *sac7* mutation (G. Chen and C. Chan, unpubl.). These results suggest that Sac7 (and Bag7), and not Bem2, may be the major GAP for Rho1 in vivo.

What then is the major in vivo function of Bem2? Several lines of evidence point toward a positive role of Bem2 in the function of Cdc42, or in the function of a protein whose function overlaps that of Cdc42. First, the phenotype of *bem2* mutants is similar to that of *cdc42* mutants (see introductory section). Second, increased dosage of *MSB1* suppresses the phenotype of *cdc42* as well as *bem2* mutants (Bender and Pringle 1989, 1991). Third, the phenotype of *bem2* mutant cells is exacerbated by loss-of-function mutations in *BEM3* or *RGA1* (*DBM1*) (Chen et al. 1996) and is suppressed by increased dosage of *BEM3* (Bender and Pringle 1991). *BEM3* and *RGA1* encode GAPs for Cdc42 (Zheng et al. 1994; Stevenson et al. 1995). Fourth, the phenotype of *bem2* mutant cells is suppressed by increased dosage of *GIC1* and *GIC2,* which encode putative effectors of Cdc42

(this study). One possible interpretation of these results is that Bem2 functions in vivo as a GAP for Cdc42, and that cycling between the GTP- and GDP-bound states is important for some aspects of Cdc42 function. However, we have not been able to detect physical association between the GAP domain of Bem2 and GTP- or GDP-bound forms of Cdc42 in the two-hybrid assay (G. Chen and C. Chan, unpubl.). Furthermore, increased dosage of *CDC42* fails to suppress the phenotype of *bem2* cells (Kim et al. 1994). Thus, details of the functional relationship between Bem2 and Cdc42 remain to be determined.

Materials and Methods

Strains, media, and genetic techniques

The yeast strains used in this study are listed in Table 1. The diploid strain CBY1830-51 was constructed by a one-step gene disruption procedure (Rothstein 1983), replacing one of the two *GIC1* genes in DBY1830 with the *gic1-Δ1::LEU2* allele present on the ~4.4-kb *Xho*I–*Sac*I fragment of pCC878. The diploid strains CBY1830-51-1 and CBY1830-51-2 were similarly constructed, replacing one of the two *GIC2* genes in CBY1830-51 with the *gic2-1::HIS3* allele present on the ~4.2-kb *Pvu*II fragment of pCC968 and with the *gic2-Δ2::TRP1* allele present on the ~2.6-kb *Kpn*I–*Sac*I fragment of pCC998, respectively. The strain CBY1830-51-1-1 was constructed by replacing one of the two *CLA4* genes in CBY1830-51-1 with the *cla4-Δ101::URA3* allele present on the ~2.5-kb *Eco*RI–*Xba*I fragment of pCC1077. These gene disruptions were confirmed by DNA hybridization. The *Escherichia coli* strain DB1142 (*leu pro thr hsdR hsdM recA*) was used routinely as a host for plasmids.

Yeast genetic manipulations as well as the preparation of rich medium (YEPD), synthetic minimal medium (SD), and SD with necessary supplements were performed as described (Rose et al. 1990). Quantitative mating assay was carried out according to established procedures (Sprague 1991). Two-hybrid assay was carried out essentially as described (Finley and Brent 1994).

Table 1. *Yeast strains used in this study*

Strain		Genotype
DBY1830	**a**/α	*ade2/+ lys2-801/+ his3-Δ200/his3-Δ200 ura3-52/ura3-52 leu2-3,112/leu2-3,112 trp1-1/trp1-1*
CBY1830-51	**a**/α	*ade2/+ lys2-801/+ his3-Δ200/his3-Δ200 ura3-52/ura3-52 leu2-3,112/leu2-3,112 trp1-1/trp1-1 gic1-Δ1::LEU2/+*
CBY1830-51-1	**a**/α	*ade2/+ lys2-801/+ his3-Δ200/his3-Δ200 ura3-52/ura3-52 leu2-3,112/leu2-3,112 trp1-1/trp1-1 gic1-Δ1::LEU2/+ gic2-1::HIS3/+*
CBY1830-51-2	**a**/α	*ade2/+ lys2-801/+ his3-Δ200/his3-Δ200 ura3-52/ura3-52 leu2-3,112/leu2-3,112 trp1-1/trp1-1 gic1-Δ1::LEU2/+ gic2-Δ2::TRP1/+*
CBY1830-51-1-1	**a**/α	*ade2/+ lys2-801/+ his3-Δ200/his3-Δ200 ura3-52/ura3-52 leu2-3,112/leu2-3,112 trp1-1/trp1-1 gic1-Δ1::LEU2/+ gic2-1::HIS3/+ cla4-Δ101::URA3/+*
RFY206	**a**	*lys2Δ201 his3-Δ200 ura3-52 leu2-3,112 trp1Δ::hisG*
EGY48	α	*his3 ura3-52 trp1 leu2::3Lexop–LEU2*
CCY71-9C-1	α	*lys2-801 his3-Δ200 ura3-52 bem2-101*
CCY311-17A	**a**	*his3-Δ200 ura3-52 leu2-3,112 trp1-1*
CCY404-2D	**a**	*lys2-801 his3-Δ200 ura3-52 leu2-3,112 trp1-1 bud5::URA3*
CCY441-52D	α	*his3-Δ200 ura3-52 leu2-3,112 trp1-1*
CCY766-9D	**a**	*lys2-801 his3-Δ200 ura3-52 leu2-3,112 trp1-1*
CCY896-8B	**a**	*his3-Δ200 ura3-52 leu2-3,112 cdc42-1*
CCY1024-19C	α	*his3-Δ200 ura3-52 leu2-3,112 trp1-1 gic1-Δ1::LEU2 gic2-1::HIS3*
CCY1027-6A	**a**	*his3-Δ200 ura3-52 leu2-3,112 cdc42-1 gic2-1::HIS3*
CCY1027-11D	**a**	*his3-Δ200 ura3-52 leu2-3,112 cdc42-1 gic1-Δ1::LEU2 gic2-1::HIS3*
CCY1027-24A	**a**	*his3-Δ200 ura3-52 leu2-3,112 cdc42-1 gic1-Δ1::LEU2*
CCY1030-6D	**a**	*his3-Δ200 ura3-52 leu2-3,112 trp1-1 bem2-Δ110::TRP1 gic2-1::HIS3*
CCY1030-10C	**a**	*his3-Δ200 ura3-52 leu2-3,112 trp1-1 bem2-Δ110::TRP1 gic1-Δ1::LEU2*
CCY1030-11B	α	*his3-Δ200 ura3-52 leu2-3,112 trp1-1 bem2-Δ110::TRP1*
CCY1030-28D	**a**	*his3-Δ200 ura3-52 leu2-3,112 trp1-1 bem2-Δ110::TRP1 gic1-Δ1::LEU2 gic2-1::HIS3*
CCY1032-2B	**a**	*his3-Δ200 ura3-52 leu2-3,112 cdc24-2 gic1-Δ1::LEU2 gic2-1::HIS3*
CCY1032-3A	**a**	*his3-Δ200 ura3-52 leu2-3,112 cdc24-2 gic2-1::HIS3*
CCY1032-6B	**a**	*his3-Δ200 ura3-52 leu2-3,112 cdc24-2 gic1-Δ1::LEU2*
CCY1032-16B	α	*his3-Δ200 ura3-52 leu2-3,112 cdc24-2*
CCY1033-5A	**a**	*his3-Δ200 ura3-52 leu2-3,112 trp1-1 gic2-1::HIS3*
CCY1033-5D	**a**	*his3-Δ200 ura3-52 leu2-3,112 trp1-1 gic1-Δ1::LEU2 gic2-1::HIS3*
CCY1033-11B	**a**	*his3-Δ200 ura3-52 leu2-3,112 trp1-1 gic1-Δ1::LEU2*
CCY1048-11A	**a**	*lys2-801 his3-Δ200 ura3-52 leu2-3,112 trp1-1 bud3-Δ101::LEU2*
CCY1055-4C	**a**	*ade2 his3-Δ200 ura3-52 leu2-3,112 trp1-1 gic1-Δ1::LEU2 gic2-1::HIS3 cla4-Δ101::URA3*
CCY1055-12B	**a**	*ade2 his3-Δ200 ura3-52 leu2-3,112 trp1-1 gic2-1::HIS3 cla4-Δ101::URA3*
CCY1055-16C	**a**	*ade2 his3-Δ200 ura3-52 leu2-3,112 trp1-1 gic1-Δ1::LEU2 cla4-Δ101::URA3*
CCY1056-6A	**a**	*ade2 his3-Δ200 ura3-52 leu2-3,112 trp1-1 cla4-Δ101::URA3*

Most of the yeast strains were constructed specifically for this study, the exceptions being DBY1830, which is from D. Botstein's laboratory collection (Stanford University, Palo Alto, CA), and EGY48 and RFY206, which are from R. Brent's laboratory collection (Harvard Medical School, Boston, MA).

Isolation of GIC1 *and* GIC2

bem2-101 ura3-52 mutant yeast cells (CCY71-9C-1) were transformed with a yeast genomic library constructed in the high copy number *URA3* plasmid YEp24 (Carlson and Botstein 1982). Ura^+ transformants were selected by plating cells on supplemented SD lacking uracil. After 24 hr at 26°C, plates containing Ura^+ transformants were shifted to 37°C. After 3 more days, Ts^+ Ura^+ transformants were identified and plasmids were recovered into *E. coli* from such transformants. The ability of these plasmids to complement the Ts^- phenotype of *bem2-101* mutant at 35 or 37°C was retested. Of ~22,000 Ura^+ transformants screened, four classes of plasmids were identified. One class (of 19 plasmids) contained, as expected, the *BEM2* gene. Another class, represented by the single *GIC1* plasmid pCC391, could complement the Ts^- phenotype of *bem2-101* mutant efficiently at 35°C and very weakly at 37°C.

The *GIC2* gene was subcloned from cosmid 9740 (gift of M. Johnston, Washington University, St. Louis, MO), using available DNA sequence information of the *GIC2* region.

DNA manipulation

pCC878, carrying the *gic1-Δ1::LEU2* mutant allele, was constructed by replacing the DNA sequence between the *Bam*HI and *Sph*I sites present in the low copy number *URA3* plasmid pCC843 with the ~2-kb *Bam*HI–*Sph*I fragment (containing *LEU2*) of pJJ283 (Jones and Prakash 1990). pCC968, carrying the *gic2-1::HIS3* mutant allele, was constructed by inserting the ~1.7-kb *Bam*HI fragment (containing *HIS3*) of pJJ215 (Jones and Prakash 1990) into the unique *Bam*HI site of the low copy number *URA3* plasmid pCC966. pCC998, carrying the *gic2-Δ2::TRP1* mutant allele, was constructed by replacing the DNA sequence between the *Bam*HI and *Pst*I sites present in the pCC966-derived low copy number *TRP1* plasmid pCC997 with the ~0.8-kb *Bam*HI–*Pst*I fragment (containing *TRP1*) of pJJ281 (Jones and Prakash 1990). The *CLA4* gene was amplified by PCR from genomic DNA of yeast strain S288C, using CLA4.1p and CLA4.2p as primers (all primers used are listed in Table 2). The ~3.6-kb *Bgl*II–*Eco*RI fragment derived from the PCR product was cloned into the *Bam*HI–*Eco*RI sites of pUC19 and pSM217, thus generating pCC1075 and pCC1079, respectively. pCC1077, carrying the *cla4-Δ101::URA3* mutant allele, was constructed by replacing the DNA sequence between the *Xho*I sites present in pCC1075 with the ~1.1-kb *Hin*dIII fragment (containing *URA3*) of pJJ244 (Jones and Prakash 1990).

Plasmids used in two-hybrid assays were constructed as follows. For pCC984, which encodes AD–Gic1, a PCR reaction was carried out with pCC904 as template and MIP23.1p and MIP23.2p as primers. The ~0.9-kb *Eco*RI–*Xho*I fragment derived from the PCR product was cloned into the *Eco*RI–*Xho*I sites of pJG4-5 (Gyuris et al. 1993). pCC985, which encodes AD–Gic2, was similarly constructed, using pCC967 as template and MIP23H.1p and MIP23H.2p as primers. The ~1.1-kb *Eco*RI fragment derived from the PCR product was cloned into the *Eco*RI site of pJG4-5. For pCC1044-1, which encodes AD–Gic1-2, a two-step recombinant PCR procedure was used (Horton et al. 1993). In the first step, two separate PCR reactions were carried out with pCC904 as template, using the primers MIP23.1p and MIP23.4p in one reaction, and the primers MIP23.2p and MIP23.3p in the other reaction. In the second step, a PCR reaction was carried out with the two PCR products from the first step as templates, using the primers MIP23.1p and MIP23.2p. The ~0.9-kb *Eco*RI–*Xho*I fragment derived from the final PCR product was cloned into the *Eco*RI–*Xho*I sites of pJG4-5. pCC1066-1, which encodes AD–Gic1-Δ4, was similarly constructed, except that the primers MIP23.3p and MIP23.4p were replaced by the primers MIP23.11p and MIP23.12p, respectively. pCC1050-1, which encodes AD–Gic1-3, was similarly constructed, except that pCC1043-2 was used as template for the first PCR step, and the primers MIP23.3p and MIP23.4p were replaced by the primers MIP23.8p and MIP23.9p, respectively. pCC1081-2, which encodes LexA–$Cdc42^{T35A,C188S}$, was also constructed by a two-step recombinant PCR procedure. In the first step, pEG202–$CDC42^{C188S}$ (Simon et al. 1995) was used as template and the primers lexA.1p and CDC42.5p were used in one reaction and the primers CDC42.3p and CDC42.4p were

Table 2. *Primers used for PCR*

Primer	Sequence (5′ → 3′)[a]
CDC42.3p	GATC*GGATCCCTCGAG*CTACAAAATTGTAGA
CDC42.4p	CAGCCGACTATGTTCCAGCAGTGTTCGA
CDC42.5p	TAGTTATCGAACACTGCTGGAACATAG
CLA4.1p	GGCGCACGAGGATAGTTC
CLA4.2p	GATC*GAATTC*GAACCATCCCAGTATCTC
lexA.1p	GATTCGTCTGTTGCAGGAAG
MIP23.1p	ATGC*GGATCCGAATTC*ATGACTGAAGGAAAGAGG
MIP23.2p	AGCC*AAGCTTCTCGAG*TCAGGTATTTCGAGGAGTA
MIP23.3p	CCATTTGATTTTCACGCTATTTCGGCTGCTAATGGT
MIP23.4p	CCTTTTACCATTAGCAGCCGAAATAGCGTGAAAATC
MIP23.8p	CGCAAAACAGTCAAGTGCAGCTACACCATTTG
MIP23.9p	GAAAATCAAATGGTGTAGCTGCACTTGACTGT
MIP23.11p	CCAAAACCGCAAAACAGTCAAGT–GCTAATGGTAAAAGGGAAGAC
MIP23.12p	GTCTTCCCTTTTACCATTAGC–ACTTGACTGTTTTGCGGTTTTGG
MIP23H.1p	AGCC*AGATCTGAATTC*ATGACTAGTGCAAGTATTAC
MIP23H.2p	GCAT*TCTAGAGAATTC*TTAAGTTTGCAGGGGCTCG

[a]Sequences derived from yeast are underlined. Restriction enzyme recognition sequences are in italics. Yeast sequences missing from primers are denoted by dashes.

used in another reaction. In the second step, the two PCR products from step one were used as templates and lexA.1p and CDC42.3p were used as primers. The ~0.6-kb *Eco*RI–*Bam* HI fragment derived from the final PCR product was cloned into the *Eco*RI–*Bam* HI sites of pEG202.

Plasmids encoding GFP fusion proteins were constructed as follows. For pCC995, which encodes GFP–Gic1, a PCR reaction was carried out with pCC904 as template and MIP23.1p and MIP23.2p as primers. The ~0.9-kb *Bam* HI–*Hin*dIII fragment derived from the PCR product was cloned into the *Bam* HI–*Hin*dIII sites of pRB2138 (Doyle and Botstein 1996). pCC1065-1, which encodes GFP-Gic2, was similarly constructed, using pCC967 as template and MIP23H.1p and MIP23H.2p as primers. The ~1.1-kb *Bgl*II–*Xba*I fragment derived from the PCR product was cloned into the *Bam* HI–*Xba*I sites of pRB2138. pCC1043-2, which encodes GFP–Gic1-2, pCC1051-1, which encodes GFP–Gic1-3, and pCC1067-1, which encodes GFP–Gic1-Δ4, were constructed as described for pCC1044-1, pCC1050-1, and pCC1066-1, respectively, except that the ~0.9-kb *Bam* HI–*Hin*dIII fragment derived from the final PCR product in each case was cloned into the *Bam* HI–*Hin*dIII sites of pRB2138.

Cytological techniques

Live yeast cells grown at room temperature (~24°C) were used for observation of GFP fusion proteins. In experiments in which visualization of DNA was desired, 4′,6-diamidino-2-phenylindole (DAPI; Accurate Chemical Co., Westbury, NY) was added to the growth medium to a final concentration of 2.5 μg/ml ~30 min before observation of cells. Immunofluorescence staining of yeast cells was carried out as described (Pringle et al. 1989).

Acknowledgments

We thank Jon Mulholland, Erfei Bi, Claudio De Virgilio, Mark Johnston, Doug Johnson, Elaine Elion, and Humberto Martin for the supply of strains, antibodies, and plasmids, and Brian Haarer for comments on the manuscript. This work was supported by National Institutes of Health grant GM45185 and Advanced Research Program grant 003658-510 from The Texas Higher Education Coordinating Board.

The publication costs of this article were defrayed in part by payment of page charges. This article must therefore be hereby marked "advertisement" in accordance with 18 USC section 1734 solely to indicate this fact.

Note added in proof

The *GIC1* and *GIC2* genes have been characterized independently in the laboratories of J. Chant and M. Peter (Brown et al., this issue).

References

Adams, A.E.M. and J.R. Pringle. 1984. Relationship of actin and tubulin distribution in wild-type and morphogenetic mutant *Saccharomyces cerevisiae*. *J. Cell Biol.* **98:** 934–945.

Adams, A.E.M., D.I. Johnson, R.M. Longnecker, B.F. Sloat, and J.R. Pringle. 1990. *CDC42* and *CDC43,* two additional genes involved in budding and the establishment of cell polarity in the yeast *Saccharomyces cerevisiae*. *J. Cell Biol.* **111:** 131–142.

Amberg, D.C., J.E. Zahner, J.W. Mulholland, J.R. Pringle, and D. Botstein. 1997. Aip3p/Bud6p, a yeast actin-interacting protein that is involved in morphogenesis and the selection of bipolar budding sites. *Mol. Biol. Cell* **8:** 729–753.

Ayscough, K.R., J. Stryker, N. Pokala, M. Sanders, P. Crews, and D.G. Drubin. 1997. High rates of actin filament turnover in budding yeast and roles for actin in establishment and maintenance of cell polarity revealed using the actin inhibitor latrunculin-A. *J. Cell Biol.* **137:** 399–416.

Bender A. and J.R. Pringle. 1989. Multicopy suppression of the *cdc24* budding defect in yeast by *CDC42* and three newly identified genes including the *ras*-related gene *RSR1*. *Proc. Natl. Acad. Sci.* **86:** 9976–9980.

———. 1991. Use of a screen for synthetic lethal and multicopy suppressee mutants to identify two new genes involved in morphogenesis in *Saccharomyces cerevisiae*. *Mol. Cell. Biol.* **11:** 1295–1305.

Bender, L., H.S. Lo, H. Lee, V. Kokojan, J. Peterson, and A. Bender. 1996. Associations among PH and SH3 domain-containing proteins and Rho-type GTPases in yeast. *J. Cell Biol.* **133:** 879–894.

Benton, B.K., A.H. Tinkelenberg, D. Jean, S.D. Plump, and F.R. Cross. 1993. Genetic analysis of Cln/Cdc28 regulation of cell morphogenesis in budding yeast. *EMBO J.* **12:** 5267–5275.

Bi, E. and J.R. Pringle. 1996. *ZDS1* and *ZDS2,* genes whose products may regulate Cdc42p in *Saccharomyces cerevisiae*. *Mol. Cell. Biol.* **16:** 5264–5275.

Brown, J.L., M. Jaquenoud, M.-P. Gulli, J. Chant, and M. Peter. 1997. Novel Cdc42-binding proteins Gic1 and Gic2 control cell polarity in yeast. *Genes & Dev.* (this issue).

Burbelo, P.D., D. Drechsel, and A. Hall. 1995. A conserved binding motif defines numerous candidate target proteins for both Cdc42 and Rac GTPases. *J. Biol. Chem.* **270:** 29071–29074.

Carlson, M. and D. Botstein. 1982. Two differentially regulated mRNAs with different 5′ ends encode secreted and intracellular forms of yeast invertase. *Cell* **28:** 145–154.

Chan, C.S.M. and D. Botstein. 1993. Isolation and characterization of chromosome-gain and increase-in-ploidy mutants in yeast. *Genetics* **135:** 677–691.

Chant, J. and I. Herskowitz. 1991. Genetic control of bud site selection in yeast by a set of gene products tht constitute a morphogenetic pathway. *Cell* **65:** 1203–1212.

Chant, J. and J.R. Pringle. 1995. Patterns of bud-site selection in the yeast *Saccharomyces cerevisiae*. *J. Cell Biol.* **129:** 751–765.

Chant, J., K. Corrado, J.R. Pringle, and I. Herskowitz. 1991. Yeast *BUD5,* encoding a putative GDP-GTP exchange factor, is necessary for bud site selection and interacts with bud formation gene *BEM1*. *Cell* **65:** 1213–1224.

Chant, J., M. Mischke, E. Mitchell, I. Herskowitz, and J.R. Pringle. 1995. Role of Bud3p in producing the axial budding pattern of yeast. *J. Cell Biol.* **129:** 767–778.

Chen, G.-C., L. Zheng, and C.S.M. Chan. 1996. The LIM domain-containing Dbm1 GTPase-activating protein is required for normal cellular morphogenesis in *Saccharomyces cerevisiae*. *Mol. Cell. Biol.* **16:** 1376–1390.

Cvrcková, F., C. De Virgilio, E. Manser, J.R. Pringle, and K. Nasmyth. 1995. Ste20-like protein kinases are required for normal localization of cell growth and for cytokinesis in budding yeast. *Genes & Dev.* **9:** 1817–1830.

Doyle, T. and D. Botstein. 1996. Movement of yeast cortical actin cytoskeleton visualized *in vivo*. *Proc. Natl. Acad. Sci.* **93:** 3886–3891.

Evangelista, M., K. Blundell, M.S. Longtine, C.J. Chow, N. Adames, J.R. Pringle, M. Peter, and C. Boone. 1997. Bni1p, a yeast formin linking Cdc42p and the actin cytoskeleton during polarized morphogenesis. *Science* **276:** 118–122.

Finley, R.L. and R. Brent. 1994. Interaction mating reveals binary and ternary connections between *Drosophila* cell cycle regulators. *Proc. Natl. Acad. Sci.* **91:** 12980–12984.

Gyuris, J., E. Golemis, H. Chertkov, and R. Brent. 1993. Cdi1, a human G1 and S phase protein phosphatase that associates with Cdk2. *Cell* **75:** 791–803.

Heim, R., A.B. Cubitt, and R.Y. Tsien. 1995. Improved green fluorescence. *Nature* **373:** 663–664.

Horton, R.M., S.N. Ho, J.K. Pullen, H.D. Hunt, Z. Cai, and L.R. Pease. 1993. Gene splicing by overlap extension. *Methods Enzymol.* **217:** 270–279.

Johnson, D.I. and J.R. Pringle. 1990. Molecular characterization of *CDC42,* a *Saccharomyces cerevisiae* gene involved in the development of cell polarity. *J. Cell. Biol.* **111:** 143–152.

Jones, J.S. and L. Prakash. 1990. Yeast *Saccharomyces cerevisiae* selectable markers in pUC18 polylinkers. *Yeast* **6:** 363–366.

Kilmartin, J. and A.E.M. Adams. 1984. Structural rearrangements of tubulin and actin diring the cell cycle of the yeast *Saccharomyces. J. Cell Biol.* **98:** 922–933.

Kim, Y.-J., L. Francisco, G.-C. Chen, E. Marcotte, and C.S.M. Chan. 1994. Control of cellular morphogenesis by the Ipl2/Bem2 GTPase-activating protein: Possible role of protein phosphorylation. *J. Cell Biol.* **127:** 1381–1394.

Lew, D.J. and S.I. Reed. 1993. Morphogenesis in the yeast cell cycle: Regulation by Cdc28 and cyclins. *J. Cell Biol.* **120:** 1305–1320.

Li, R., Y. Zheng, and D.G. Drubin. 1995. Regulation of cortical actin cytoskeleton assembly during polarized cell growth in budding yeast. *J. Cell Biol.* **128:** 599–615.

Martin, H., A. Mendoza, J.M. Rodriguez-Pachón, M. Molina, and C. Nombela. 1997. Characterization of *SKM1,* a *Saccharomyces cerevisiae* gene encoding a novel Ste20/PAK-like protein kinase. *Mol. Microbiol.* **23:** 431–444.

Matsui, Y., R. Matsui, R. Akada, and A. Toh-e. 1996. Yeast *src* homology region 3 domain-binding proteins involved in bud formation. *J. Cell Biol.* **133:** 865–878.

Park, H.-O., E. Bi, J.R. Pringle, and I. Herskowitz. 1997. Two active states of the Ras-related Bud1/Rsr1 protein bind to different effectors to determine yeast cell polarity. *Proc. Natl. Acad. Sci.* **94:** 4463–4468.

Peterson, J., Y. Zheng, L. Bender, A. Myers, R. Cerione, and A. Bender. 1994. Interactions between the bud emergence proteins Bem1p and Bem2p and Rho-type GTPases in yeast. *J. Cell Biol.* **127:** 1395–1406.

Pringle, J.R., R.A. Preston, A. Adams, T. Stearns, D. Drubin, B.K. Haarer, and E. Jones. 1989. Fluorescence microscopy methods for yeast. *Methods Cell Biol.* **31:** 357–435.

Roemer, T., L.G. Vallier, and M. Snyder. 1996. Selection of polarized growth sites in yeast. *Trends Cell Biol.* **6:** 434–441.

Rose, M.D., F. Winston, and P. Hieter. 1990. *Methods in yeast genetics.* Cold Spring Harbor Laboratory Press, Cold Spring Harbor, NY.

Rothstein, R.J. 1983. One-step gene disruption in yeast. *Methods Enzymol.* **101:** 202–211.

Ruggieri, R., A. Bender, Y. Matsui, S. Powers, Y. Takai, J.R. Pringle, and K. Matsumoto. 1992. RSR1, a *ras*-like gene homologous to K*rev*-1 (*sm g21A/rap1A*): Role in the development of cell polarity and interactions with the Ras pathway in *Saccharomyces cerevisiae. Mol. Cell. Biol.* **12:** 758–766.

Schmidt, A., M. Bickle, T. Beck, and M.N. Hall. 1997. The yeast phosphatidylinositol kinase homolog TOR2 activates RHO1 and RHO2 via the exchange factor ROM2. *Cell* **88:** 531–542.

Simon, M.-N., C. De Virgilio, B. Souza, J.R. Pringle, A. Abo, and S.I. Reed. 1995. Role for the Rho-family GTPase Cdc42 in yeast mating-pheromone signal pathway. *Nature* **376:** 702–705.

Sloat, B.F. and J.R. Pringle. 1978. A mutant of yeast defective in cellular morphogenesis. *Science* **200:** 1171–1173.

Sloat, B.F., A. Adams, and J.R. Pringle. 1981. Roles of the *CDC24* gene product in cellular morphogenesis during the *Saccharomyces cerevisiae* cell cycle. *J. Cell Biol.* **89:** 395–405.

Sprague, G.F. 1991. Assay of yeast mating reaction. *Methods Enzymol.* **194:** 77–93.

Stevenson, B.J., B. Ferguson, C. De Virgilio, E. Bi, J.R. Pringle, G. Ammerer, and G.F. Sprague. 1995. Mutation of *RGA1,* which encodes a putative GTPase-activating protein for the polarity-establishment protein Cdc42p, activates the pheromone response pathway in the yeast *Saccharomyces cerevisiae. Genes & Dev.* **9:** 2949–2963.

Sutton, A., D. Immanuel, and K.T. Arndt. 1991. The *SIT4* protein phosphatase functions in late G1 for progression into S phase. *Mol. Cell. Biol.* **11:** 2133–2148.

Symons, M., J.M.J. Derry, B. Karlak, S. Jiang, V. Lemahieu, F. McCormick, U. Francke, and A. Abo. 1996. Wiskott-Aldrich syndrome protein, a novel effector for the GTPase CDC42Hs, is implicated in actin polymerization. *Cell* **84:** 723–734.

Wang, T. and A. Bretscher. 1995. The *rho*-GAP encoded by *BEM2* regulates cytoskeletal structure in budding yeast. *Mol. Biol. Cell.* **6:** 1011–1024.

Yamochi, W., K. Tanaka, H. Nonaka, A. Maeda, T. Mucha, and Y. Takai. 1994. Growth site localization of Rho1 small GTP-binding protein and its involvement in bud formation in *Saccharomyces cerevisiae. J. Cell Biol.* **125:** 1077–1093.

Zahner, J.E., H.A. Harkins, and J.R. Pringle. 1996. Genetic analysis of the bipolar pattern of bud site selection in the yeast *Saccharomyces cerevisiae. Mol. Cell. Biol.* **16:** 1857–1870.

Zhao, Z.-S., T. Leung, E. Manser, and L. Lim. 1995. Pheromone signaling in *Saccharomyces cerevisiae* requires the small GTP-binding protein Cdc42p and its activator CDC24. *Mol. Cell. Biol.* **15:** 5246–5257.

Zheng, Y., M.J. Hart, K. Shinjo, T. Evans, A. Bender, and R.A. Cerione. 1993. Biochemical comparisons of the *Saccharomyces cerevisiae* Bem2 and Bem3 proteins. *J. Biol. Chem* **268:** 24629–24634.

Zheng, Y., R. Cerione, and A. Bender. 1994. Control of the yeast bud-site assembly GTPase Cdc42: Catalysis of guanine-nucleotide exchange by Cdc24 and stimulation of GTPase activity by Bem3. *J. Biol. Chem.* **269:** 2369–2372.

Zheng, Y., A. Bender, and R.A. Cerione. 1995. Interaction among proteins involved in bud-site assembly in *Saccharomyces cerevisiae. J. Biol. Chem.* **270:** 626–630.

Ziman, M. and D.I. Johnson. 1994. Genetic evidence for a functional interaction between *Saccaromyces cerevisiae CDC24* and *CDC42. Yeast* **10:** 463–474.

Ziman, M., J.M. O'Brien, L.A. Ouellette, W.R. Church, and D.I. Johnson. 1991. Mutational analysis of *CDC42Sc,* a *Saccharomyces cerevisiae* gene that encodes a putative GTP-binding protein involved in the control of cell polarity. *Mol. Cell. Biol.* **11:** 3537–3544.

Ziman, M., D. Preuss, J. Mulholland, J.M. O'Brien, D. Botstein, and D.I. Johnson. 1993. Subcellular localization of Cdc42p, a *Saccharomyces cerevisiae* GTP-binding protein involved in the control of cell polarity. *Mol. Biol. Cell* **4:** 1307–1316.

The Cdc42 GTPase-associated proteins Gic1 and Gic2 are required for polarized cell growth in *Saccharomyces cerevisiae*

Guang-Chao Chen, Yung-Jin Kim and Clarence S.M. Chan

Genes Dev. 1997, **11:**
Access the most recent version at doi:10.1101/gad.11.22.2958